PHOTOACOUSTICS MODELING WITH COMSOL MULTIPHYSICS

Patrick Grahn

COMSOL Oy
Arabiankatu 12
00560 Helsinki
patrick@comsol.fi

Abstract

Photoacoustic devices are playing an increasingly important role in biological, medical and spectroscopic applications. They utilize the excitation of pressure waves by light, connecting the fields of acoustics and photonics. Using mathematical models, we can improve our understanding of the interplay between multiple physical phenomena in the device's geometry, which allows us to optimize its performance. In this article, we review the theoretical principle of the photoacoustic effect and demonstrate its application by using a simulation model of a photoacoustic sensor.

1 INTRODUCTION

The use of photoacoustic techniques has been rapidly increasing in many applications of photoacoustic imaging [1] and trace gas analysis [2]. Numerical modeling with COMSOL Multiphysics is often used for the design and product development of a wide range of photoacoustics applications [3-8]. Modeling enables a quantitative characterization of the acoustical, thermal, mechanical and optical properties of a system. The obtained knowledge can decrease the need of physical prototypes and improve existing designs.

In this paper, we present the theory of optically excited pressure waves that is necessary for modeling of photoacoustics applications. We also create a COMSOL model of a cantilever-based photoacoustic sensor, commonly used for detection and analysis of gases. The model is solved using a combination of thermoviscous acoustics and geometrical optics. We analyze the results of the workflow, proceeding from the exciting laser beam, all the way to the interferometric readout.

2 MATHEMATICAL DESCRIPTION

Acoustics signals are small pressure variations in a fluid with a large background pressure. The governing equations are derived by linearizing the Navier-Stokes equations, continuity equation and energy equation. In frequency domain, we may express the resulting linearized equations as follows:

$$\mathrm{j}\omega\rho_0\mathbf{u} = -\nabla p + \nabla\cdot\left(\mu[\nabla\mathbf{u} + (\nabla\mathbf{u})^{\mathrm{T}}] - \left[\tfrac{2}{3}\mu - \mu_{\mathrm{B}}\right][\nabla\cdot\mathbf{u}]\tilde{\mathbf{I}}\right), \quad (1)$$

$$\mathrm{j}\omega\rho + \rho_0\nabla\cdot\mathbf{u} = 0, \quad (2)$$

$$\mathrm{j}\omega\rho_0 C_p T = \nabla\cdot(k\nabla T) + \mathrm{j}\omega p T_0\alpha_0 + Q, \quad (3)$$

$$\rho = \rho_0(\beta_T p - \alpha_0 T), \quad (4)$$

where we have added the fluid's equation of state as the fourth equation. The unknown small-signal quantities are the acoustic pressure p, velocity $\mathbf{u}$, temperature T and fluid density ρ. Given the material properties of the fluid, these four quantities may be solved from the set of equations above. This is done by using COMSOL's thermoviscous acoustics interface. More details on the material properties and their connection to the speed of sound is discussed in an earlier article on thermoviscous acoustics modeling [9]. In contrast to the earlier article, we have included a term Q in the energy equation that describes a time-harmonic heat source. Its units is W/m^3. This source term is the key for modeling photoacoustics.

Photoacoustics considers the excitation of acoustic pressure by light. Consider light propagation through a gas or liquid. Light may interact with the fluid through two common mechanisms. First, the electric-field component of light polarizes the molecules of the fluid, which radiate a secondary electric field. This effect slows down light propagation in the medium and is characterized by the real part of the fluid's refractive index. Second, photons may be absorbed by molecular or electronic transitions in the fluid. The energy absorbed may be re-radiated by spontaneous or stimulated emission, but in many cases, the excited molecules decay to the ground state by a non-radiative process, converting the absorbed energy to heat. This second mechanism causes the intensity of a light beam to decrease upon propagation in the fluid. This effect is commonly accounted by the imaginary part of the fluid's refractive index.

From Eq. (3), it is clear that a time-harmonic oscillation of a heat-source will create a time-harmonic pressure in a fluid. In order for a beam of light to create such a heat source, two criterions must be met. First, the optical frequency should match an available molecular or electronic transition. An efficient way to achieve this, is to use a laser source with the frequency tuned in-resonance with a known transition. Second, we must modulate the heat source in time. This can be done by amplitude modulation of the light, for example, using a mechanical chopper. Alternatively, for laser beams we may employ frequency modulation. Shifting the optical frequency tunes the beam out-of-resonance with a molecular resonance.

The time-dependent modulated heat source may be expressed in terms of the optical variables as

$$Q_{\mathrm{time}} = 2\frac{\omega_{\mathrm{opt}}}{c_0}\mathrm{Im}\{n\}I, \quad (5)$$

where I is the optical intensity, n the complex-valued refractive index, ω_{opt} the optical angular frequency and c_0 the speed of light in vacuum. From Eq. (5), we see that amplitude modulation corresponds to varying I, whereas frequency modulation corresponds to vary-

ing Im$\{n\}$. Both methods achieve the same effect of making the heat source time-dependent. In the simplest case, we could consider a sinusoidal modulation of the optical intensity $I(t) = I_0(1 + \cos(\omega t))$. Inserting this into Eq. (5) and transforming to frequency domain yields the following source for thermoviscous acoustics

$$Q = 2\frac{\omega_{\text{opt}}}{c_0}\text{Im}\{n\}I_0. \quad (6)$$

The intensity distribution I_0 may be solved by COMSOL's Geometrical Optics interface.

3 MODEL OF A PHOTOACOUSTIC SENSOR

As an example of application, we construct a model of a cantilever-based photoacoustic sensor. Photoacoustic sensors enable detection of very low concentrations of molecules in fluids. This is because the photoacoustic signal is directly related to the absorbed energy by the target molecules. The considered sensor is cantilever-based, with the photoacoustic signal being measured interferometrically from the displacement of a silicon cantilever. This method gives superior sensitivity and linearity compared to sensors utilizing traditional condenser microphones [10].

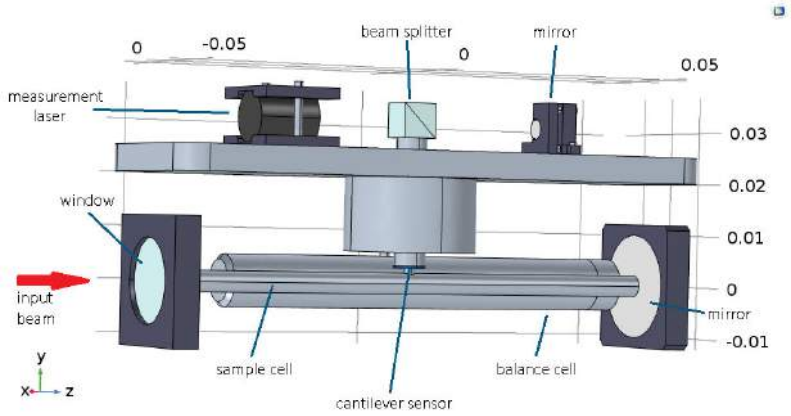

Figure 1. Geometry used in the simulation. A modulated input beam generates an acoustic signal in the sample cell. The pressure variation between the sample and balance cell causes a micrometer-sized cantilever to oscillate. This oscillation is measured with a laser in a Michelson interferometer, where the cantilever acts as a mirror.

The geometry of the sensor, created using COMSOL CAD tools, is shown in Figure 1. Some of the system parameters are adapted from Ref. [11], which uses a detector provided by Gasera Ltd. The operation principle is that a light beam enters the sample cell through the window on the left. The end-mirror reflects the beam, such that it passes the cell twice. The sample cell contains an unknown amount of substance to be sensed. The optical frequency of the input beam has been tuned to an absorption resonance of the substance. By modulation of the source, a time-harmonic heat source is created that, in turn, gives rise to

an acoustic field. The pressure difference between the sample cell and a balance cell exerts a force on a cantilever actuator. This force is proportional to the imaginary part of the fluid's refractive index and, thus, proportional to the concentration of the unknown substance. The displacement of the cantilever is measured optically, using a Michelson interferometer.

Modeling the operation of the photoacoustic sensor may be divided into three parts. First, we perform ray tracing of the incident light beam through the sample cell and determine the acoustic heat source. Second, we solve the thermoviscous acoustics in the fluid coupled with solid mechanics in the cantilever and substrate. The bidirectional coupling between acoustics and mechanics is automatically done in COMSOL. Finally, we perform a second ray tracing simulation for the measurement laser beam and compute the intensity distributions created by the interferometer.

In this example, we consider the sample gas to consist of Argon with a small concentration of Carbon dioxide (CO_2) to be detected. The simulation parameters for the gases are taken from Ref. [11]. The gas is at standard conditions for temperature and pressure, which corresponds to a molecular density of $2.7{\cdot}10^{25}$ 1/m^3 for Argon. The wavelength of the used laser light is tuned at 1572.018 nm, matching an absorption line of CO_2 characterized by a molecular absorption cross section of $7.5{\cdot}10^{-27}$ m^2. Let us consider a case, where the CO_2 concentration is 100 ppm, corresponding to a molecular density of $2.7{\cdot}10^{21}$ 1/m^3. From the wavelength, cross section and molecular density, the imaginary part of the refractive index is calculated to be $5{\cdot}10^{-12}$.

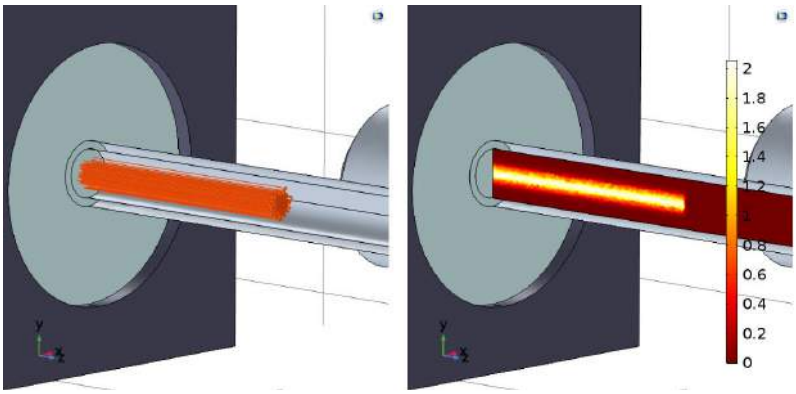

Figure 2. Computation of optical heat source. The light beam is divided into a distribution of discrete rays that are traced through the cell (left image). The rays are shown at an arbitrary time during the ray tracing. They propagate from left to right. The colored slice plot (right image) shows the heat loss in W/m^3 that is recorded in the volume by the rays.

Computed ray trajectories of the used 30 mW laser beam are shown in Figure 2. The light beam was assumed to have a Gaussian shape and anti-reflection coating was applied to the cell window. The beam shown in Figure 2 eventually reaches the end-mirror (see Figure 1) and gets reflected back through the cell. Consequently, the final heat source Q will have a maximum power density of about 4 W/m^3 at the center of the beam. The total power lost

to heat is about 0.24 μW. As a combination of the short optical path length and small CO_2 concentration, the light beam is only weakly attenuated after passing through the sample cell.

In the next step, we simulate the acoustic fields created by the optical heat source Q. Thermoviscous acoustics is solved in the Argon gas domains, with the following material properties: ρ_0 = 1.78 kg/m^3, μ = 22.4·10^{-6} Pa·s, μ_B = 0, C_p = 0.52·10^3 J/(kg·K), k = 17.4·10^{-3} W/(m·K), $\alpha_0 = 1/T_0$, $\beta_T = 1/p_0$. For the solid mechanics part, the silicon cantilever has a length of 5 mm, width of 2 mm and 10 μm thickness. The 10 μm cantilever layer is separated from a 380 μm silicon substrate by a 1 μm thick SiO2 layer.

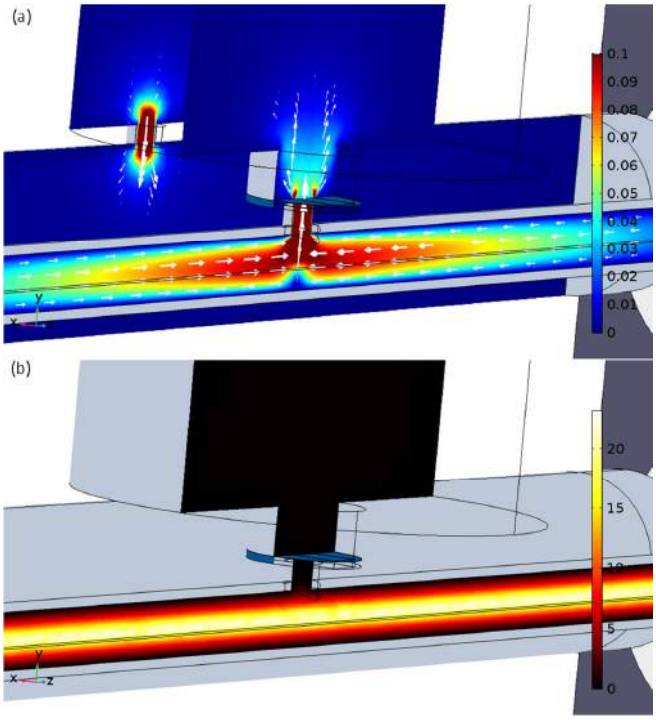

Figure 3. Slice plots of the acoustic fields for a laser beam modulated at 10 Hz. Figure (a) shows the velocity field in μm/s. Planes through both the sample and balance cell are shown. Figure (b) shows the temperature field in μK in the sample cell. The colors indicate the peak value of the time-harmonic fields.

Considering amplitude modulation of the laser beam at 10 Hz, the calculated thermoviscous fields are shown in Figure 3. The acoustic temperature field is localized along the path of the optical heat source. The velocity field, on the other hand, is strongest in narrow ducts and around the cantilever. The thermal and viscous dissipation damp the oscillation of the cantilever. The difference in acoustic pressure across the cantilever was evaluated to be about 0.3 mPa.

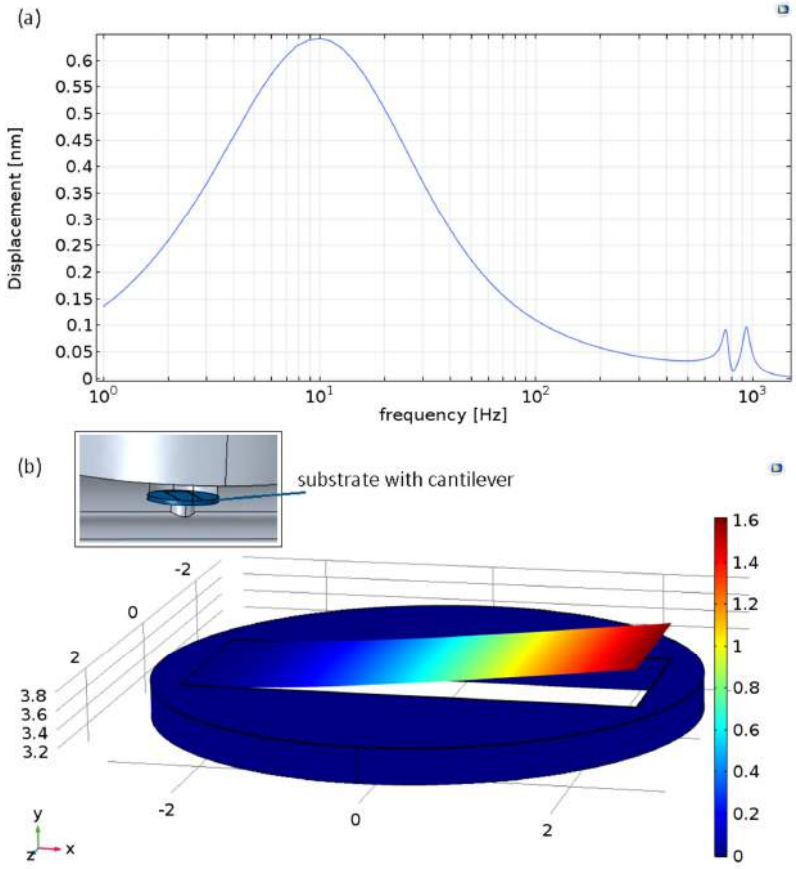

Figure 4. (a) Cantilever displacement amplitude as a function of modulation frequency (volume averaged). (b) Cantilever displacement field in nm at 10 Hz. The shown geometrical deformation is scaled for visualization. The small inset shows the location of the cantilever in the geometry.

A sweep of modulation frequencies was carried out. For an input power amplitude of 30 mW, the displacement amplitude as a function of modulation frequency is shown in Figure 4(a). The figure shows that the chosen frequency of 10 Hz is quite optimal for the used geometry. For frequencies above 10 Hz, the pressure generated by the heat source decreases inversely proportional to the frequency. This decrease may be understood using Eq. (3), which indicates that the generated p is proportional to Q/ω. This proportionality holds, when we are outside the thermal boundary layer and $\nabla \cdot (k\nabla T)$ may be neglected. For frequencies below 10 Hz, the thermal boundary layer thickness becomes comparable to the diameter of the sample cell and, therefore, heat is lost to the walls by the conduction term $\nabla \cdot (k\nabla T)$. Additionally, at low frequencies, the acoustic pressure leaks through the small gap between the cantilever and its frame. These two effects both reduce the generated

cantilever displacement. The two peaks seen at 750 Hz and 950 Hz correspond to the resonance of the cantilever's fundamental mode, coupled with the acoustic field. Higher-order cantilever modes are not present in the considered frequency range. In our case, the cantilever oscillates as shown in Figure 4(b).

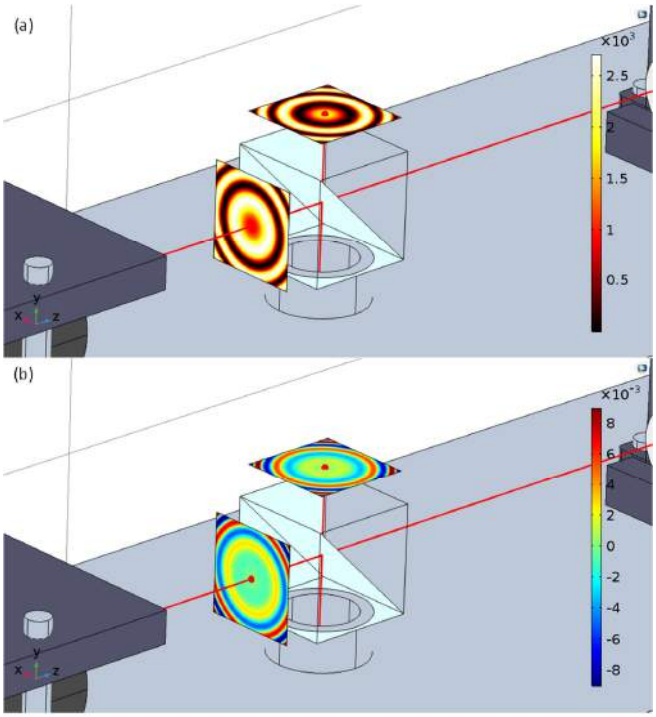

Figure 5. (a) Interference patterns formed by the interferometer. The intensity in W/m^2 is shown with a thermal colormap. (b) Differential interference signal obtained by subtracting the patterns at maximum and null cantilever displacement.

Using the solved displacement field of the cantilever, we perform the ray tracing simulation in the interferometer. The cantilever acts as an oscillating mirror. A wavelength of 600 nm was used for the laser and the wavefront's radius of curvature was initialized to obtain focus on the surface of the cantilever. In Figure 5(a), the interference patterns in the case of no displacement are shown. The small displacement of the cantilever causes a small shift to this interference pattern. Figure 5(b) shows the difference between the patterns for maximum displacement amplitude and null displacement. This difference is the sensor's signal. By positioning photodetectors at appropriate locations, electronics can extract the signal from the measured intensity. Although, the solution here was obtained for a displacement on the order of one nanometer, further optimized interferometers combined with appropriate signal processing schemes may resolve even sub-picometer displacements [12].

4 CONCLUSIONS

We have shown how the heat source obtained with optical ray tracing can be used for thermoviscous acoustics modeling. Using COMSOL Multiphysics, we have simulated a cantilever-based photoacoustic sensor system. It is seen that the cantilever performance is influenced by several factors, such as modulation frequency and thermoviscous damping. The results indicate that components' geometrical sizes and shapes may have a decisive impact on the system performance. Using the presented model, one can further improve and optimize the sensor design in terms of signal strength and stability.

REFERENCES

[1] Beard P, "Biomedical photoacoustic imaging", Interface Focus 1 (2011), 602-631.

[2] Patimisco P, Scamarcio G, Tittel F K, Spagnolo V, "Quartz-Enhanced Photoacoustic Spectroscopy: A Review", Sensors 14 (2014), 6165-6206.

[3] C Sowmiya, Thittai A K, "Simulation of photoacoustic tomography (PAT) system in COMSOL® and comparison of two popular reconstruction techniques", Proc. SPIE 10137 (2017).

[4] Upputuri P K, Wen Z-B, Wu Z, Pramanik M, "Super-resolution photoacoustic microscopy using photonic nanojets: a simulation study", Journal of Biomedical Optics 19 (2014).

[5] Hatef A, Darvish B, Sajjadi A Y, "Computational study of plasma-assisted photoacoustic response from gold nanoparticles irradiated by off-resonance ultrafast laser", J. Nanopart. Res. 19 (2017).

[6] Ishaku L A, Hutson D, "A Resonant Photoacoustic CO_2 Sensor Based on MIR-IR LED and MEMS Microphone Technology Operating at 4.3μm", Innovative Systems Design and Engineering 7 (2016).

[7] Wolff M, Kost B, Baumann B, "Shape-Optimized Photoacoustic Cell: Numerical Consolidation and Experimental Confirmation", Int. J. Thermophys. 33 (2012), 1953-1959.

[8] Zeninari V, Vallon R, Risser C, Parvitte B, "Photoacoustic Detection of Methane in Large Concentrations with a Helmholtz Sensor: Simulation and Experimentation", Int. J. Thermophys. 37 (2016).

[9] Grahn P, "Thermoacoustics modeling of loudspeakers with COMSOL Multiphysics", Proceedings of the Acoustical Society of Finland (2015). http://www.akustinenseura.fi/wp-content/uploads/2015/09/AP2015_Paperin_palautus_34.pdf

[10] Uotila J, "Use of the Optical Cantilever Microphone in Photoacoustic Spectroscopy", (Doctoral thesis, University of Turku, 2009).

[11] Koskinen V, Fonsen J, Roth K, Kauppinen J, "Cantilever enhanced photoacoustic detection of carbon dioxide using a tunable diode laser source", Appl. Phys. B. 86 (2007).

[12] Kauppinen I, "Optical audio microphone arrangement including a Michelson type interferometer for providing a phase difference between different parts of light beams", US Patent 7,521,668 (2009).